J|A|C|S ARTICLES

Published on Web 06/17/2010

E-Type Delayed Fluorescence of a Phosphine-Supported $Cu_2(\mu\text{-}NAr_2)_2$ Diamond Core: Harvesting Singlet and Triplet Excitons in OLEDs[||]

Joseph C. Deaton,*[,†] Steven C. Switalski,[†] Denis Y. Kondakov,[†] Ralph H. Young,[†] Thomas D. Pawlik,[†] David J. Giesen,[†] Seth B. Harkins,[‡] Alex J. M. Miller,[‡] Seth F. Mickenberg,[§] and Jonas C. Peters*[,‡]

Eastman Kodak Company, Rochester, New York 14650, Division of Chemistry and Chemical Engineering, California Institute of Technology, Pasadena, California 91125, and Department of Chemistry, Massachusetts Institute of Technology, Cambridge, Massachusetts 02139

Received January 18, 2010; E-mail: jdeaton1@rochester.rr.com; jpeters@caltech.edu

Abstract: A highly emissive bis(phosphine)diarylamido dinuclear copper(I) complex (quantum yield = 57%) was shown to exhibit E-type delayed fluorescence by variable temperature emission spectroscopy and photoluminescence decay measurement of doped vapor-deposited films. The lowest energy singlet and triplet excited states were assigned as charge transfer states on the basis of theoretical calculations and the small observed S_1-T_1 energy gap. Vapor-deposited OLEDs doped with the complex in the emissive layer gave a maximum external quantum efficiency of 16.1%, demonstrating that triplet excitons can be harvested very efficiently through the delayed fluorescence channel. The function of the emissive dopant in OLEDs was further probed by several physical methods, including electrically detected EPR, cyclic voltammetry, and photoluminescence in the presence of applied current.

Introduction

Since the pioneering work on organic light-emitting diodes (OLEDs) comprising amorphous thin films by scientists at Eastman Kodak Company,[1,2] the technology has been vigorously pursued for application in flat-panel displays and energy-efficient lighting.[3] To achieve the maximum device efficiency, luminescent materials capable of converting the formally spin-forbidden triplet excitons as well as singlet excitons into useful light output are needed. Phosphorescent complexes of heavy atoms that possess large spin−orbit coupling interactions can overcome the spin-forbidden nature of the triplet to singlet ground state transition.[4] Presently, the leading candidates appear to be cyclometalated iridium(III) complexes, of which tris(2-phenylpyridinato-$\hat{N}C^{2'}$-)iridium(III), $Ir(ppy)_3$, is the prototype.[5−9] Devices doped with Ir complexes have been reported to have external quantum efficiencies (EQE, photons per electron) in the range of 20−29% with no optical outcoupling enhancements.[10−14] To our knowledge, there have been no reports of OLEDs containing complexes of common metals as emitters that produce such high efficiencies, despite the cost and supply advantages that common metals would offer.

The luminescence behavior of copper(I) complexes is rich,[15−17] but quantum yields are usually low. Some complexes exhibit

[†] Eastman Kodak Company.
[‡] California Institute of Technology.
[§] Massachusetts Institute of Technology.
[||] Work carried out at Eastman Kodak Company, Rochester, New York 14650, was done prior to December, 2009.

(1) Tang, C. W.; Van Slyke, S. A. *Appl. Phys. Lett.* **1987**, *51*, 913–915.
(2) Tang, C. W.; Van Slyke, S. A.; Chen, C. H. *J. Appl. Phys.* **1989**, *65*, 3610–3616.
(3) (a) Hatwar, T. K.; Kondakova, M. E.; Giesen, D. J.; Spindler, J. P. In *Organic Electronics: Materials, Processing, Devices and Applications*; So, F., Ed.; CRC Press: Boca Raton, FL, 2009; pp 433−509. (b) Hatwar, T. K; Spindler, J. P. In *Luminescent Materials and Applications*; Kitai, A., Ed.; John Wiley & Sons: Hoboken, NJ, 2008; pp 111−159. (c) So, F.; Kido, J.; Burrows, P. *MRS Bull.* **2008**, *3*, 663–669. (d) Kondakova, M. E.; Deaton, J. C.; Pawlik, T. D.; Giesen, D. J.; Kondakov, D. Y.; Young, R. H.; Royster, T. L.; Comfort, D. L.; Shore, J. D. *J. Appl. Phys.* **2010**, *107*, 014515-1-13.
(4) Yersin, H. *Top. Curr. Chem.* **2004**, *241*, 1–26.
(5) Baldo, M. A.; Lamansky, S.; Burrows, P. E.; Thompson, M. E.; Forrest, S. R. *Appl. Phys. Lett.* **1999**, *75*, 4–6.
(6) Lamansky, S.; Djurovich, P.; Murphy, D.; Abdel-Razzaq, F.; Lee, H. E.; Adachi, C.; Burrows, P. E.; Forrest, S. R.; Thompson, M. E. *J. Am. Chem. Soc.* **2001**, *123*, 4304–4312.
(7) Lamansky, S.; Djurovich, P.; Murphy, D.; Abdel-Razzaq, F.; Kwong, R.; Tsyba, I.; Bortz, M.; Mui, B.; Bau, R.; Thompson, M. E. *Inorg. Chem.* **2001**, *40*, 1704–1711.
(8) Hack, M.; Weaver, M. S.; Adamovich, V.; Kwong, R. C.; Lu, M. H.; Brown, J. J. *Proc. SPIE* **2005**, *5961*, 596102−1−9.
(9) Djurovich, P. I.; Thompson, M. E. In *Highly Efficient OLEDs with Phosphorescent Materials*; Yersin, H. H., Ed.; Wiley-VCH Verlag GmbH & Co., KgaA: Weinheim, Germany, 2008.
(10) Adachi, C.; Baldo, M. A.; Thompson, M. E.; Forrest, S. R. *J. Appl. Phys.* **2001**, *90*, 5048–5051.
(11) Kondakova, M. E.; Pawlik, T. D.; Young, R. H.; Giesen, D. J.; Kondakov, D. Y.; Brown, C. T.; Deaton, J. C.; Lenhard, J. R.; Klubek, K. P. *J. Appl. Phys.* **2008**, *104*, 094501-1-17.
(12) Chopra, N.; Lee, J.; Zheng, Y.; Eom, S.-H.; Xue, J.; So, F. *Appl. Phys. Lett.* **2008**, *93*, 143307-1-3.
(13) Tanaka, D.; Agata, Y.; Sasabe, S.; Li, Y.-J.; Su, S.-J.; Takeda, T.; Kido, J. *Jpn. J. Appl. Phys.* **2007**, *46*, L10–L12.
(14) Tanaka, D.; Agata, Y.; Takeda, T.; Watanabe, S.; Kido, J. *Jpn. J. Appl. Phys.* **2007**, *46*, L117–L119.
(15) Armaroli, N.; Accorsi, G.; Cardinali, F.; Listorti, A. *Top. Curr. Chem.* **2007**, *280*, 69–115.
(16) Ford, P. C.; Cariati, E.; Bourassa, J. *Chem. Rev.* **1999**, *99*, 3625–3647.
(17) (a) Ford, P. C. *Coord. Chem. Rev.* **1994**, *132*, 129–140. (b) Yam, V. W. W.; Lo, K. K. W.; Fung, W. K. M.; Wang, C. R. *Coord. Chem. Rev.* **1998**, *171*, 17–41.

two independent emissions with different decay times.[18−21] These observations have been interpreted with a model in which emission arises from two triplet states that do not readily interconvert because they arise from different orbital parentages.[18−21] In contrast, Kirchhoff et al.[22] concluded from the temperature dependence of emission from $Cu(dmp)_2^+$ (dmp = 2,9-dimethyl-1,10-phenanthroline) that it arises from two excited states that interconvert readily by intersystem crossing: a triplet and a singlet in thermal equilibrium. Through addition of steric groups to hinder distortions in the excited states, the luminescence quantum yields of Cu(I) phenanthroline complexes were increased up to 16%.[23−28]

In 2005, Harkins and Peters reported the highly emissive complex bis(bis(diisobutylphenylphosphino)amido) dicopper(I), $[Cu(PNP)]_2$, having a solution quantum yield (68%) and long lifetime (10.2 μs) that are unprecedented among copper(I) complexes.[29] These physical properties make this an interesting new class of compounds to explore in OLEDs for display and lighting applications. A key feature of these emissive dicopper complexes that likely contributes to their favorable emission properties concerns low overall structural reorganization between their ground and emissive excited states. Strong covalency in the Cu_2N_2 core that houses a redox active molecular orbital (RAMO) can provide a mechanism for transferring charge from the dicopper(I) ground state to a structurally similar emissive excited state, as modeled by comparing the dicopper(I) ground state geometric and electronic structure to its one- and even two-electron oxidized ground state structures.[30] While less thoroughly studied, mononuclear copper(I) complexes having phosphinoamido ligands were reported by Miller et al. that possess similar quantum yields and lifetimes, likely for similar reasons.[31]

The long lifetimes of these new dicopper (and monocopper) emitters appear to be suggestive of phosphorescent emission from a triplet state. However, anomalously small Stokes shifts stand in contrast to this suggestion. We now show that the room temperature emission of a close analogue of the originally communicated dicopper emitter, $[Cu(PNP\text{-}^tBu)]_2$ (Scheme 1), is dominated by E-type (thermally activated) delayed fluorescence. To the best of our knowledge, this complex possesses

Scheme 1

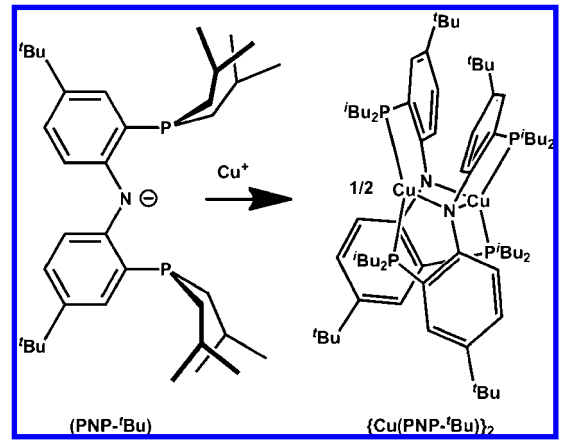

the highest solution quantum yield of any system that luminesces via the E-type delayed fluorescence mechanism. The material is thermally stable and sublimable, unlike many emissive copper(I) complexes, and thus is not limited to solution processing, but can also be vapor-deposited. We have thereby been able to demonstrate the use of this material to harvest singlet and triplet excitons in vapor-deposited OLEDs via the delayed fluorescence channel. The maximum EQE of 16.1% was substantially higher than any other reported value we know for OLEDs employing emitters other than complexes of the platinum group metals such as iridium. In addition, mechanistic aspects of the doped devices have been probed by electrically detected electron paramagnetic resonance (EDEPR), cyclic voltammetry (CV), and photoluminescence (PL) in the presence of applied current.

Experimental Section

$[Cu(PNP\text{-}^tBu)]_2$ was synthesized by the published procedure.[30] The methods and instrumentation used for the following measurements and procedures were described previously in the references cited: vapor pressures,[32] solution quantum yield and decay time,[29] prompt and delayed emission spectra,[32] vapor-deposited films and OLED fabrication and evaluation,[32] cyclic voltammetery,[33] and electrically detected electron paramagnetic resonance.[11,34] Steady-state emission spectra of vapor-deposited films were recorded as previously described,[35] except the excitation source was the 458 nm line of an Ar ion laser, while the excitation spectra were recorded using a xenon arc lamp source and Cary-14 monochromator. Luminescence decay at variable temperatures was obtained as previously described,[35] except the excitation source was a coumarin-450 dye laser pumped by a YAG laser and tuned to 460 nm.

Density functional theory (DFT) calculations were performed on $[Cu(PNP\text{-}^tBu)]_2$ using the B3LYP[36,37] method. The ground state geometry and orbitals were calculated using the Jaguar[38] program with the MIDI![39] basis set on H, C, N, and P atoms and the

(18) Kyle, K. R.; Ryu, C. K.; DiBenedetto, J. A.; Ford, P. C. *J. Am. Chem. Soc.* **1991**, *113*, 2954–2965.
(19) Ryu, C. K.; Vitale, M.; Ford, P. C. *Inorg. Chem.* **1993**, *32*, 869–874.
(20) Buckner, M. T.; Matthews, T. G.; Lytle, F. E.; McMillin, D. R. *J. Am. Chem. Soc.* **1979**, *101*, 5846–5848.
(21) Casadonte, D. J.; McMillin, D. R. *J. Am. Chem. Soc.* **1987**, *109*, 331–337.
(22) Kirchhoff, J. R.; Gamache, R. E., Jr.; Blaskie, M. W.; Del Paggio, A. A.; Lengel, R. K.; McMillin, D. R. *Inorg. Chem.* **1983**, *22*, 2380–2384.
(23) Eggleston, M. K.; McMillin, D. R.; Koenig, K. S.; Pallenberg, A. J. *Inorg. Chem.* **1997**, *36*, 172–176.
(24) Miller, M. T.; Gantzel, P. K.; Karpishin, T. B. *J. Am. Chem. Soc.* **1999**, *121*, 4292–4293.
(25) Cuttell, D. G.; Kuang, S. M.; Fanwick, P. E.; McMillin, D. R.; Walton, R. A. *J. Am. Chem. Soc.* **2002**, *124*, 6–7.
(26) Kuang, S. M.; Cuttell, D. G.; McMillin, D. R.; Fanwick, P. E.; Walton, R. A. *Inorg. Chem.* **2002**, *41*, 3313–3322.
(27) Felder, D.; Nierengarten, J.-F.; Barigelletti, F.; Ventura, B.; Armaroli, N. *J. Am. Chem. Soc.* **2001**, *123*, 6291–6299.
(28) Kalsani, V.; Schmittel, M.; Listorti, A.; Accorsi, G.; Armaroli, N. *Inorg. Chem.* **2006**, *45*, 2061–2067.
(29) Harkins, S. B.; Peters, J. C. *J. Am. Chem. Soc.* **2005**, *127*, 2030–2031.
(30) Harkins, S. B.; Mankad, N. P.; Miller, A. J. M.; Szilagyi, R. K.; Peters, J. C. *J. Am. Chem. Soc.* **2008**, *130*, 3478–3485.
(31) Miller, A. J. M.; Dempsey, J. L.; Peters, J. C. *Inorg. Chem.* **2007**, *46*, 7244–7246.
(32) Deaton, J. C.; Place, D. W.; Brown, C. T.; Rajeswaran, M.; Kondakova, M. E. *Inorg. Chim. Acta* **2008**, *361*, 1020–1035.
(33) Kondakov, D. Y.; Sandifer, J. R.; Tang, C. W.; Young, R. H. *J. Appl. Phys.* **2003**, *93*, 1108–1119.
(34) Pawlik, T. D.; Kondakova, M. E.; Giesen, D. J.; Deaton, J. C.; Kondakov, D. Y. *J. Soc. Info. Display* **2009**, *17*, 279–286.
(35) Marchetti, A. P.; Deaton, J. C.; Young, R. Y. *J. Phys. Chem. A* **2006**, *110*, 9828–9838.
(36) Becke, A. D. *Phys. Rev.* **1988**, *38*, 3098–3100.
(37) Stephens, P. J.; Devlin, F. J.; Chabalowski, C. F.; Frisch, M. J. *J. Phys. Chem.* **1994**, *98*, 11623–11627.
(38) *Jaguar 5.5*; Schrödinger, LLC: Portland, Oregon, 2003.

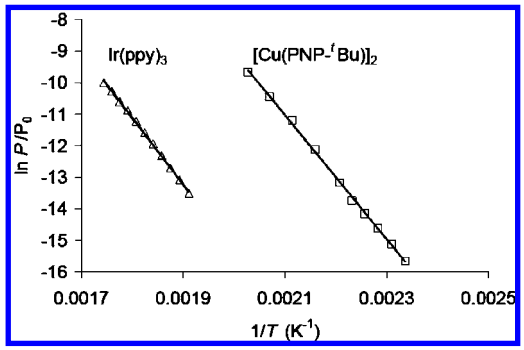

Figure 1. Temperature dependence of vapor pressures determined by the Knudsen effusion technique for $Ir(ppy)_3$ and $[Cu(PNP\text{-}^tBu)]_2$.

LACV3P[38,40] basis set and pseudopotential on the Cu atoms. Time-dependent density functional theory (TD-DFT)[41−43] was used on this geometry to calculate the excited state orbital character using the B3LYP method with the MIDI! basis set on H, C, N, and P atoms and with the LANL2DZ[40,44,45] basis set and pseudopotential on the Cu atoms. The TD-DFT calculations were done with Gaussian03.[46]

Host and transport materials used in the fabrication of devices were synthesized at Eastman Kodak Company or were purchased commercially.

The electroluminescence (EL) spectrum of an OLED at 77 K was obtained by placing the OLED horizontally in a wide-mouth dewar flask, positioning an optical fiber over the emissive area, and immersing in liquid nitrogen. The optical fiber led to a diode array spectrophotometer, and the spectrum was recorded after the boiling of the liquid nitrogen had subsided.

Excitation light for PL of devices was provided by a 300 W xenon arc lamp, an Oriel Cornerstone 260 1/4 m monochromator, and a 450 nm bandpass filter and focused onto an OLED at 45° relative to the device plane. The luminescence perpendicular to the device plane was recorded through an appropriate Corning long-pass filter using a PhotoResearch PR650 Spectrascan Colorimeter. Current was applied to the OLED using a Keithley constant current source while the PL or simultaneous PL and EL, if any, was measured.

Results and Discussion

Sublimation. The vapor pressure of $[Cu(PNP\text{-}^tBu)]_2$ at various temperatures was measured by the Knudsen effusion technique[32,47] and is shown in Figure 1 compared to that of $Ir(ppy)_3$. The enthalpy and entropy of sublimation for the median temperature of measurement ($\Delta_{sub}H_m$ and $\Delta_{sub}S_m$, respectively) were calculated from a linear fit to the experimental data using the integrated form of the Clausius−Clayperon, eq 1 ($P_0 = 1$ atm, R = gas constant). The values are listed in Table 1.

$$\ln(P/P_0) = \Delta_{sub}S_m/R - \Delta_{sub}H_m/RT \qquad (1)$$

Table 1. Enthalpy and Entropy of Sublimation for $[Cu(PNP\text{-}^tBu)]_2$ and $Ir(ppy)_3$

Compound	T_m (K)	$\Delta_{sub}H_m$ (kJ mol^{-1})	$\Delta_{sub}S_m$ (J K^{-1} mol^{-1})
$[Cu(PNP\text{-}^tBu)]_2$	460	163.8 ± 1.8	252.3 ± 4.0
$Ir(ppy)_3$	548	175.8 ± 1.8	224.1 ± 3.2

$[(Cu(PNP\text{-}^tBu)]_2$ was sublimed in bulk in a tube furnace with nitrogen entrainment gas at 195 °C. When a sample was prepurified by recrystallization, the sublimation proceeded very cleanly, leaving little ash or residue in the sublimation boat. The original $[Cu(PNP)]_2$ complex was found to sublime at approximately the same temperature under similar conditions. By comparison, $Ir(ppy)_3$ sublimed at ∼290 °C under similar conditions and rate. The utility of the present dinuclear copper complexes should therefore not be limited to solution-processed OLEDs but should be suitable for vapor-deposited OLEDs.

Photophysical Properties. Solution absorption and emission spectra for $[Cu(PNP\text{-}^tBu)]_2$ are shown in Figure 2a. The spectra are very similar to those previously reported[29] for $[Cu(PNP)]_2$. The quantum yield (57%) and decay time (11.5 μs) are also similar to the values previously reported[29] for $[Cu(PNP)]_2$ (68% and 10.2 μs, respectively). The lowest energy absorption region appears to comprise at least two overlapping bands. The extinction coefficients (5601 M^{-1} cm^{-1} at 433 nm and 4203 M^{-1} cm^{-1} at 463 nm) are too high for triplet absorptions and are in the range normally assigned as singlet MLCT transitions. No weak absorptions that could be assigned to spin-forbidden triplet states are seen in the present spectrum, indicating that those triplet absorptions either are not resolved from the singlet absorption or are too weak to be detected at this concentration. The luminescence decay time is similar to that of triplet state emission in heavy atom complexes, such as cyclometalated Pt(II) complexes, in which strong spin−orbit coupling interactions enable rapid singlet−triplet intersystem crossing as well as intensity from the otherwise spin-forbidden phosphorescence.[48,49] However, the apparent Stokes shift of the $[Cu(PNP\text{-}^tBu)]_2$ emission appears to be too small for a triplet emission given that the triplet state is always lower than the corresponding singlet state observed in the absorption.

To better understand the nature of the emitting state(s), the temperature dependence of the emission was examined. To avoid complication by any solvent phase change, the complex was doped into evaporated amorphous films for these studies. Through experimentation with several hosts, 1,1-bis(4-(*N*,*N*-di-*p*-tolylamino)phenyl)cyclohexane (TAPC) was selected as an inert host material for the evaporated films to avoid crystallization of the films. A 200 Å undoped layer of TAPC was first deposited onto a quartz disk, followed by 2000 Å of TAPC doped with 1% $[Cu(PNP\text{-}^tBu)]_2$, and finally an 800 Å capping layer of undoped TAPC.

Excitation and emission spectra of the doped film at 295 and 100 K are shown in Figure 2b. The excitation spectra correspond closely to the low energy portion of the solution absorption spectrum, and the two overlapping bands are more clearly resolved. (Only the low energy portion of the excitation spectrum was recorded to avoid host absorption and possible photochemical degradation.) The emission spectra gradually shifted to a longer wavelength as the temperature was lowered as far as 100 K, below which no further shift was observed.

(39) Easton, R. E.; Giesen, D. J.; Welch, A.; Cramer, C. J.; Truhlar, D. G. *Theor. Chim. Acta* **1996**, *93*, 281–301.
(40) Hay, P. J.; Wadt, W. R. *J. Chem. Phys.* **1985**, *82*, 299–310.
(41) Stratmann, R. E.; Scuseria, G. E.; Frisch, M. J. *J. Chem. Phys.* **1998**, *109*, 8128–8224.
(42) Bauernschmitt, R.; Ahlrichs, R. *Chem. Phys. Lett.* **1996**, *256*, 454–464.
(43) Casida, M. E.; Jamorski, C.; Casida, K. C.; Salahub, D. R. *J. Chem. Phys.* **1998**, *108*, 4439–4449.
(44) Hay, P. J.; Wadt, W. R. *J. Chem. Phys.* **1985**, *82*, 270–283.
(45) Hay, P. J.; Wadt, W. R. *J. Chem. Phys.* **1985**, *82*, 284–298.
(46) Frisch, M. J. *Gaussian 03*, revision B.05 ed.; Gaussian, Inc: Pittsburgh, PA, 2003.
(47) Knudsen, M. *Ann. Phys.* **1909**, *28*, 999–1016.
(48) Yersin, H.; Donges, D. *Top. Curr. Chem.* **2001**, *214*, 81–186.
(49) Brooks, J.; Babayan, Y.; Lamansky, S.; Djurovich, P. I.; Tsyba, I.; Bau, R.; Thompson, M. E. *Inorg. Chem.* **2002**, *41*, 3055–3066.

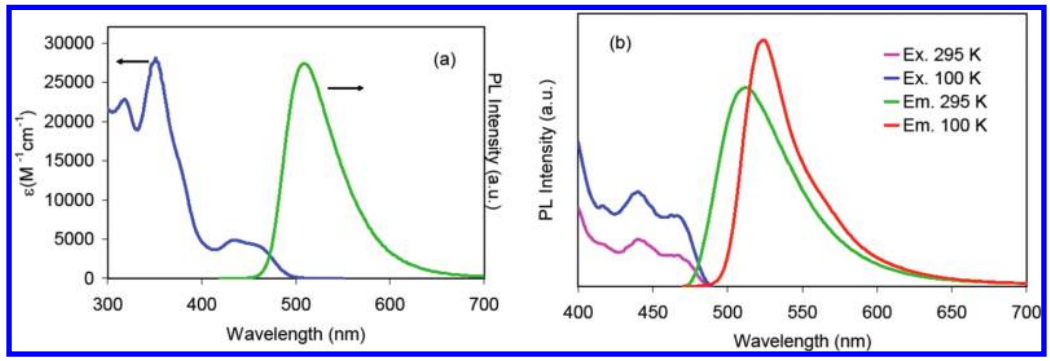

Figure 2. (a) Absorption and emission of $[Cu(PNP\text{-}^tBu)]_2$ in 2-MeTHF solution at 295 K. (b) Excitation and emission spectra at 295 and 100 K of the vapor-deposited film structure TAPC (200 Å) | TAPC + 1% $[Cu(PNP\text{-}^tBu)]_2$ (2000 Å) | TAPC (800 Å) on quartz substrate. Excitation spectra were collected with detection at 524 nm, and emission spectra were collected for excitation with the 458 nm line of an Ar ion laser.

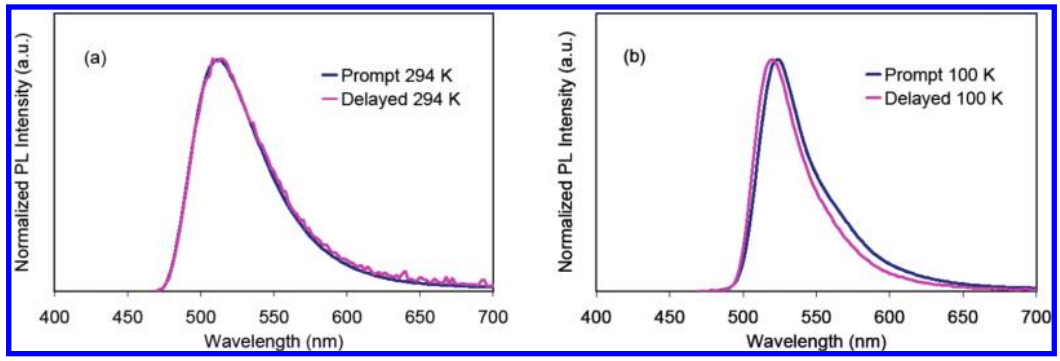

Figure 3. Prompt and delayed emission spectra at (a) 294 K and (b) 100 K for the vapor-deposited film structure TAPC (200 Å) | TAPC + 1% $[Cu(PNP\text{-}^tBu)]_2$ (2000 Å) | TAPC (800 Å) on quartz substrate. Excitation was by the 458 nm line of an Ar ion laser.

The excitation spectra, however, did not shift with temperature. Therefore, the emission bands observed at room temperature and low temperature arise from two excited states belonging to the same complex. The higher energy emission band observed at room temperature crosses over the excitation spectrum, while the lower energy band observed at low temperature has a larger apparent Stokes shift. The energy separation between the two emission bands was roughly estimated to be 740 cm^{-1} from the emission energies at the points on the high energy side of each band at which the intensity was 25% of the intensity at the respective peak maximum. The energy spacing between the two bands is much larger than may reasonably be attributed to a zero-field splitting (ZFS) among sublevels of a triplet state in view of the known values for a large number of transition metal complexes.[4] Therefore, the two bands arise from two different states.

To test whether the two emitting states were independent or in thermal equilibrium, time-gated spectra and decay times at different wavelengths were measured at various temperatures from 295 down to 65 K. Time-resolved spectra were acquired over a 900 μs integration period for delays of 0 (prompt) or 200 μs (delayed) after the excitation pulse. The prompt and delayed spectra at 295 K showed no difference in band shape (Figure 3a). A narrowing of the band shape was observed in the delayed spectra at lower temperatures, including intermediate temperatures where both emission bands contribute significantly as well as still lower temperatures at which only the lowest energy band contributes. This is exemplified by the prompt and delayed spectra at 100 K shown in Figure 3b. The apparent shift in peak wavelength is small relative to the energy difference between the high- and low-temperature emission bands and does not appear to be related, as it is also observed at temperatures at which the high-energy emission band is frozen out. There is no indication that the high- and low-temperature emission bands are resolved in time at intermediate temperatures where both contribute strongly. Decay times were measured with detection at wavelengths spanning the emission envelope of both states (500, 510, 520, 530, and 540 nm) at various temperatures. No significant difference in decay time was obtained for different wavelengths at a given temperature, particularly temperatures where both high- and low-temperature bands contribute strongly. Evidently the shift in the time-gated spectra as seen in Figure 3b is small enough that no significant change in decay rate was observed as a function of detecting wavelength. The above sets of experiments indicate that the two excited states responsible for the high- and low-temperature emission bands are in thermal equilibrium on the time scale of the experiment. Therefore, the temperature dependence of the luminescence decay rate may be analyzed as a Boltzmann average decay rate of the two emitting states (*vide infra*), at least down to the lowest temperature (65 K) for which the time-resolved spectra and decay times were compared.

To increase the signal for additional decay measurements, a second coating on quartz was prepared in which the thickness of the doped layer was increased to 10 000 Å and the concentration of $[Cu(PNP\text{-}^tBu)]_2$ was increased to 1.5%. This sample was capped with a 200 Å layer of undoped TAPC and was covered with a protective coating of Al.

The observed decay time (τ_{obs}) for detection at 520 nm is shown as a function of temperature in Figure 4a. Single exponential decays were obtained at temperatures from 295 down to ~30 K, but below 30 K, the decay was not single exponential. The decay appeared to be nearly single exponential again at temperatures of 4.2 and 2 K where the sample was

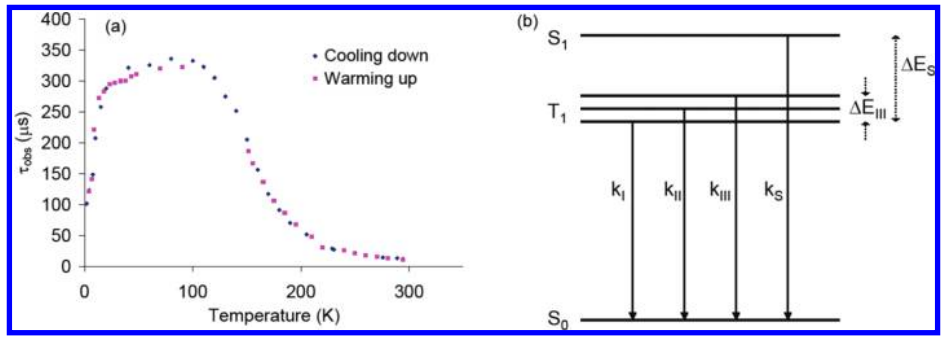

Figure 4. (a) Temperature dependence of observed luminescence decay time for the vapor-deposited film structure TAPC (200 Å) | TAPC + 1.5% [Cu(PNP-^{t}Bu)]$_2$ (10 000 Å) | TAPC (200 Å) | Al (1000 Å) on quartz substrate. Decays below 30 K were not single exponential (see text). (b) Energy level diagram for proposed two-state emission system of [Cu(PNP-^{t}Bu)]$_2$.

immersed in liquid helium. Decay times that fit the longer time portion of each decay below 30 K, which accounted for most of the integrated intensity, were selected for inclusion in Figure 4a. Local heating by the laser was checked as a possible cause of the nonsingle exponential decay below 30 K by reducing the power of the laser probe, but no change in the decay could be discerned before signal intensity became too weak.

As indicated in Figure 4a, the variation in decay time over the entire temperature range was reversible, indicating that no sample degradation or photochemistry was affecting the decay results. The decay time at room temperature, 11.3 μs, agreed well with the value measured in solution and that originally reported for [Cu(PNP)]$_2$ in cyclohexane solution.[29] As the temperature was lowered, the decay time lengthened to a maximum value of 336 μs at 80 K. There was nearly a plateau in decay time over the temperature range of approximately 60 to 110 K before the decay time shortened again as the temperature was lowered further. The decay time at 4.2 K was 124 μs, while in two measurements at 2 and 1.8 K the same value of 101 μs was recorded.

The value of 336 μs for the decay time at 80 K where only the lower energy emission band contributes clearly shows that this band arises from a triplet state. A likely assignment for the higher energy emission band based on its substantial overlap with the first absorption band and its small Stokes shift (~2070 cm^{-1}) is that it originates from the lowest singlet excited state when it is thermally populated. An energy level diagram according to the initial hypothesis of the lowest triplet and singlet states both contributing to the emission is shown in Figure 4b. As illustrated, emission may occur from each of the three sublevels of the triplet state and from the singlet state.

The observed decay rate ($k_{obs} = 1/\tau_{obs}$) for such a two-state system in thermal equilibrium may be described as a Boltzmann average by eq 2:

$$k_{obs} = \frac{k_I + k_{II}\exp(-\Delta E_{II}/kT) + k_{III}\exp(-\Delta E_{III}/kT) + k_S\exp(-\Delta E_S/kT)}{1 + \exp(-\Delta E_{II}/kT) + \exp(-\Delta E_{III}/kT) + \exp(-\Delta E_S/kT)} \quad (2)$$

The decay rates of the individual sublevels of the triplet system are k_I, k_{II}, and k_{III}, respectively; k_S is the decay rate for the singlet state, while k is the Boltzmann constant. ΔE_{II}, ΔE_{III}, and ΔE_S are the energies of the second triplet sublevel, the third triplet sublevel, and the singlet state, respectively, above the energy of the lowest triplet sublevel. Each decay rate in eq 2 is the sum of the respective radiative and nonradiative decay rates (k_r and k_{nr}, respectively). Radiative decay rates for each state or sublevel may be assumed to be temperature independent, but

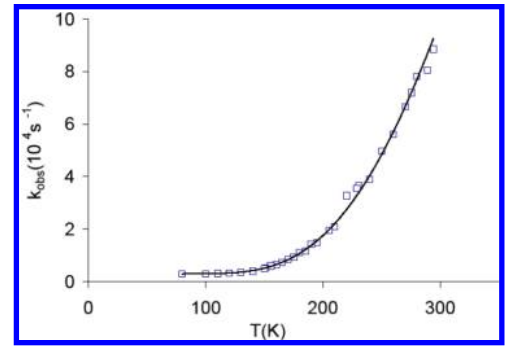

Figure 5. Observed luminescence decay rates (□) over the temperature range 80 to 294 K and the calculated decay rates (solid curve) using eq 3 with parameters $k_{ave} = 2913$ s^{-1}, $k_S = 1.27 \times 10^7$ s^{-1}, and $\Delta E_S = 786$ cm^{-1}.

nonradiative decay rates may depend on temperature. An equation analogous to eq 2 may be written for the radiative decay rate of the two-state system. The overall radiative decay rate at each temperature may in principle be determined experimentally from the product of k_{obs} and the quantum yield at each temperature because the quantum yield by definition is $k_r/(k_r + k_{nr})$. In this manner, Kirchhoff et al.[22] analyzed the *radiative* decay rates of the Cu(dmp)$_2^+$ complex having a relatively low quantum yield that was sensitive to temperature. But *observed* decay rates for triplet emission of Pt(2-thienylpyridine)$_2$[50] and Ir(ppy)$_3$[51] were analyzed using eq 2, except of course for omission of the singlet terms. For [Cu(PNP-^{t}Bu)]$_2$, the approximation that nonradiative decay rates of the singlet state and the triplet sublevels are constant with temperature is reasonable because quantum yield is already fairly high at 295 K and emission intensity at 100 K appears comparable to that at 295 K (Figure 2b). Therefore, the observed decay rates were analyzed using eq 2.

At temperatures where thermal energy is much larger than the triplet ZFS ($kT \gg \Delta E_{III}$), eq 2 simplifies to eq 3 where $k_{ave} = (k_I + k_{II} + k_{III})/3$.

$$k_{obs} = \frac{3k_{ave} + k_S\exp(-\Delta E_S/kT)}{3 + \exp(-\Delta E_S/kT)} \quad (3)$$

The observed decay rates at 80 to 295 K were fit to eq 3 by varying k_{ave}, k_S, and ΔE_S. An excellent fit (Figure 5) to the

(50) Strasser, J.; Homeier, H. H. H.; Yersin, H. *Chem. Phys.* **2000**, *255*, 301–316.
(51) Finkenzeller, W. J.; Yersin, H. *Chem. Phys. Lett.* **2003**, *377*, 299–305.

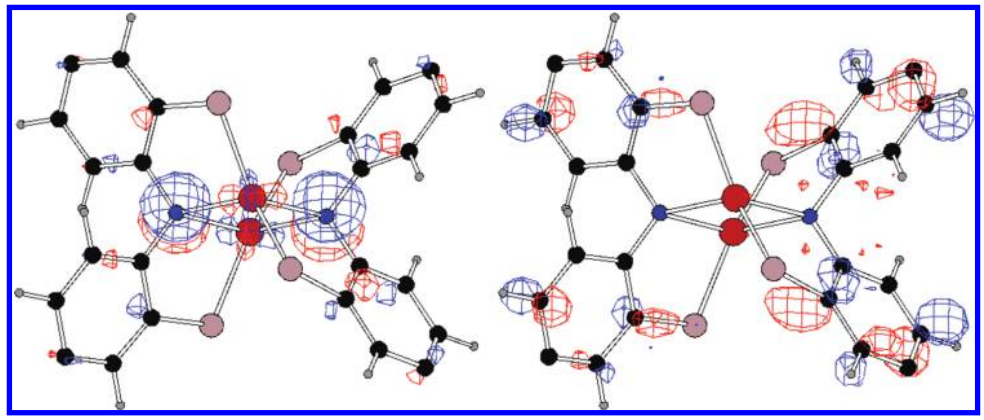

Figure 6. Calculated HOMO (left) and LUMO (right) of [Cu(PNP-^{t}Bu)]$_2$, at the T1 geometry. For clarity, the alkyl groups have been removed from the visualizations.

experimental data was obtained with values of $k_{ave} = 2913 \pm 75$ s^{-1}, $k_S = (1.27 \pm 0.09) \times 10^7$ s^{-1}, and $\Delta E_S = 786 \pm 11$ cm^{-1}. The value of ΔE_S from the fit agrees well with the estimate from the energy difference between the high- and low-temperature emission bands noted above (740 cm^{-1}). The quantum yield in the solid film may be assumed to be the same as that in solution (57%) because the decay times in the film and in solution were almost the same. This leads to an estimate of 1.66×10^3 s^{-1} for the average radiative decay rate of the triplet state and 7.24×10^6 s^{-1} for the singlet state. For comparison, Kirchhoff and co-workers deduced from variable temperature solution studies of the Cu(dmp)$_2^+$ complex that two excited states, one triplet and one singlet, are also involved in its emission.[22] The radiative decay rate constants for the triplet and singlet in that complex were estimated to be 1×10^3 and 2×10^7 s^{-1}, respectively. Using ultrafast techniques, Siddique et al.[52] determined a radiative rate constant of 2×10^6 for the prompt emission of Cu(dmp)$_2^+$, although it was noted that this value could be lower than that determined by Kirchoff et al. due to intersystem crossing to the triplet state. Siddique et al.[52] assigned the prompt emission as a singlet on the basis of the radiative decay rate being $>10^6$.

As a reviewer pointed out, obtaining a fit to the Boltzmann expression, eq 3, does not distinguish whether the upper excited state is a singlet or a second triplet. The radiative decay rate determined here for the upper excited state in [Cu(PNP-^{t}Bu)]$_2$ indicates it is a singlet. In addition, the singlet assignment may be made because the emission at room temperature crosses over the first absorption band so deeply and that absorption was assigned to a singlet excited state based on its extinction. For a triplet to have such a large radiative decay rate as determined for the upper excited state, or to have such a large extinction for ground state absorption, it would have to have an extraordinary degree of mixing with a singlet state having greater oscillator strength in its transition to or from the ground state. For a first row metal complex, this would require such a singlet state to be very near in energy to the triplet. In the absorption spectrum, there does not appear to be a more intense absorption band very close to the first absorption band, and so that band is assigned as a singlet, not as a triplet borrowing intensity from a nearby singlet. As mentioned in regard to certain other emissive copper(I) complexes,[26] there is still a possibility that a second triplet could contribute to the emission at high temperature in addition to the main contribution from the singlet excited state.

At very low temperatures where kT is no longer large relative to the triplet ZFS, the upper triplet sublevels should begin to be depopulated, resulting in further change to the Boltzmann average decay rate. However, varying the decay rate and energy spacings for the individual triplet sublevels in eq 2 did not give a physically meaningful fit to the observed increase in decay rate as the temperature was lowered from 60 to 2 K. As noted above, the decay was not single exponential below ~30 K. The assumption of thermal equilibrium as the basis for eq 2 may not be valid at low temperature. Slow spin−lattice relaxation among the triplet sublevels may be expected at low temperature for complexes with ZFS that is smaller than the lattice phonon energies of the host matrix (i.e., on the order of 0.1 cm^{-1}).[50,53] [Cu(PNP-^{t}Bu)]$_2$ very likely does have such a small ZFS, as do other metal complexes[48] with k_{ave} in a similar range, because the ZFS and decay rate have a common origin in the spin−orbit coupling interaction.

Theoretical Calculations. The HOMO and LUMO of [Cu(PNP-^{t}Bu)]$_2$ calculated by the DFT method are shown in Figure 6. The HOMO resides mainly on the four-membered Cu_2N_2 ring, in agreement with previously reported calculations showing strong covalent interaction and delocalization over the Cu and N atoms of an analogue compound.[30] The LUMO resides almost entirely on the ligand aryl groups that bridge the amido and phosphine groups. The TD-DFT calculations indicate that the first excited singlet and triplet states are both >90% HOMO→LUMO in character. This suggests that the lowest excited states are almost pure charge transfer in nature. This assignment is consistent with the small S_1 energy splitting reported in the preceding section. The TD-DFT calculations also predict a decrease in the Cu−Cu distance from 2.81 Å in the ground state to 2.61 Å in the excited state but a less than 0.05 Å change in the Cu−N bond lengths in the excited state. This relatively small overall molecular distortion in the excited state is consistent with the small Stokes shift observed in the 295 K emission and is also complementary to the previously published X-ray structure comparison that established a similarly small overall molecular structure change upon oxidation of [Cu(PNP-^{t}Bu)]$_2$ by one electron to [Cu(PNP-^{t}Bu)]$_2^+$, but with a substantial Cu−Cu compression.[30] The ground state structure of [Cu(PNP-^{t}Bu)]$_2^+$ appears to be a good structural model of the lowest excited states of [Cu(PNP-^{t}Bu)]$_2$.

(52) Siddique, Z. A.; Yamamoto, Y.; Ohno, T.; Nozaki, K. *Inorg. Chem.* **2003**, *42*, 6366–6378.

(53) Yersin, H.; J.; Strasser, J. *Coord. Chem. Rev.* **2000**, *208*, 331–364.

Table 2. Structural Formulae of Organic Host Materials

TAPC	TCTA	HPT	TPBI
mCP	CBP	2,7-DCP	2,6-DCN
SBFK	ACBP	1,5-DCN	TRAZ

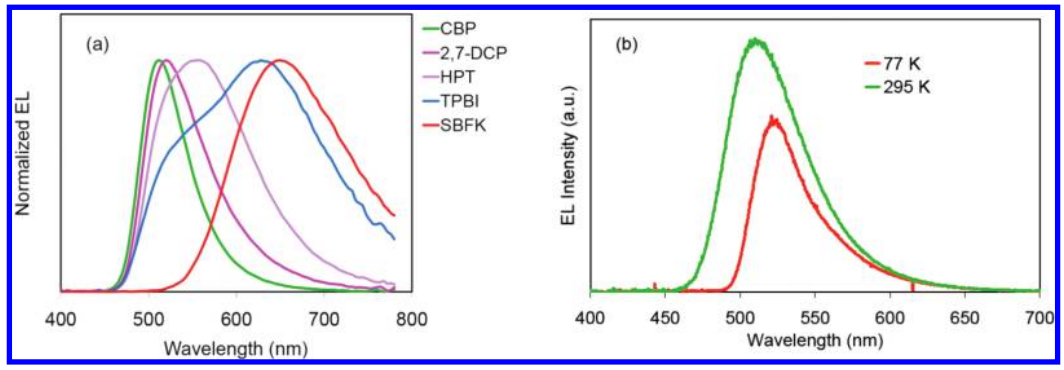

Figure 7. (a) Normalized electroluminescence spectra for devices containing 8% $[Cu(PNP\text{-}^tBu)]_2$ dopant in selected host materials. (b) Electroluminescence spectra at 295 and 77 K of a device comprising 8% $[Cu(PNP\text{-}^tBu)]_2$ doped in CBP host.

Electroluminescence. $[Cu(PNP\text{-}^tBu)]_2$ was first screened as an emissive layer dopant in a collection of diverse host materials, all having triplet energies that were found by DFT calculation[11] to be high enough that green phosphorescent emitters should not be quenched. The device formulation for these bottom-emitting coatings on a glass support consisted of the following sequence of layers or a minor variation thereof: ITO (220 Å) | CFx (10 Å) | NPB (850 Å) | TAPC (100 Å) | Host +8% $[Cu(PNP\text{-}^tBu)]_2$ (350 Å) | Bphen (500 Å) | LiF (5 Å) | Al (1200 Å), where CFx is a coating produced by plasma-assisted polymerization of CHF_3,[54] NPB is the hole-transporting material 4,4′-bis[*N*-(1-naphthyl)-*N*-phenylamino]biphenyl, and Bphen is the electron-transporting material 4,7-diphenyl-1,10-phenanthroline. The structural formulas of the host materials are listed in Table 2. Although TAPC was used as a host for the photophysical studies and other experiments (*vide infra*), it was not screened as the sole host in OLEDs because of the barrier to electron injection into the relatively high LUMO level of this dominantly hole-transporting material. For all host materials screened, the doped devices produced new EL bands with much higher efficiency than the corresponding undoped devices. Green electroluminescence was obtained with the host materials CBP, mCP, and TCTA that closely matched the PL spectrum of the $[Cu(PNP\text{-}^tBu)]_2$ dopant in the TAPC films. However, broadened and red-shifted EL was obtained with the other host materials. The normalized EL spectra of doped devices for selected hosts are compared in Figure 7a. The λ_{max} and the external quantum efficiencies (EQE) of the EL at 1 mA/cm^2 are listed in Table 3

(54) Hung, L. S.; Zheng, L. R.; Mason, M. G. *Appl. Phys. Lett.* **2001**, *78*, 673–676.

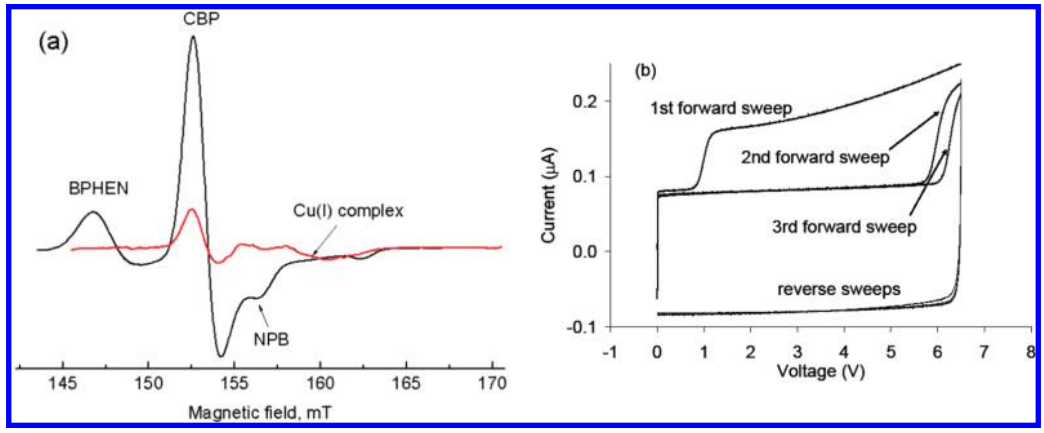

Figure 8. (a) EDEPR spectra of devices of the structure: ITO (220 Å) | CFx (10 Å) | NPB (750 Å) | TAPC (100 Å) | CBP + x% [Cu(PNP-^{t}Bu)]$_2$ (300 Å) | Bphen (500 Å) | LiF (5 Å) | Al (1200 Å) for $x = 0$% (black) and $x = 8$% (red). (b) Voltammogram of the holes-only device ITO (250 Å) | CFx (10 Å) | TAPC (750 Å) | TAPC + 1% [Cu(PNP-^{t}Bu)]$_2$ (350 Å) | TAPC (500 Å) | Al (1200 Å). Sweep rate was 50 V/s.

Table 3. Emission Maximum and EL Efficiency at 1 mA/cm^2 for Devices Containing 8% [Cu(PNP-^{t}Bu)]$_2$ Dopant in Host Materials with Various Reduction Potentials (E_{red})

Host	Host E_{red} (V vs SCE[a])	λ_{max} (nm)	EQE (% ph/e)
CBP	−2.34	512	8.76
2,7-DCP	−2.24	520	6.81
HPT	−2.13	558	6.67
2,6-DCN	−2.23	568	6.86
1,5-DCN	−2.10	587	6.92
TPBI	−2.02	628	0.43
ACBP	−1.82	602	1.02
SBFK	−1.56	649	0.35
TRAZ	−1.51	640	0.19

[a] Solutions for voltammetry were prepared in 1:1 acetonitrile/toluene containing 0.1 M tetrabutylammonium tetrafluoroborate and were deaerated with Ar prior to measurement. The Fc/Fc+ potential was measured in this solvent as 0.50 V vs SCE.

together with the solution reduction potential for each host. As the host reduction potential becomes less negative than that of CBP, the emission shifts from the green molecular [Cu(PNP-^{t}Bu)]$_2$ emission to the red. These broad emissions have the appearance of exciplex emission. Exciplexes that are charge transfer states between the dopant (donor) and host (acceptor) molecules may be expected when the oxidation potential of the dopant is relatively low (high HOMO level). The first oxidation potential of [Cu(PNP-^{t}Bu)]$_2$ is indeed very low: −490 mV vs Fc/Fc$^+$ (reversible) in THF with 0.35 M [NBu$_4$][PF$_6$].[30]

The EQEs varied strongly with the host materials as shown in Table 3. The efficiency was highest when the [Cu(PNP-^{t}Bu)]$_2$ molecular emission was obtained in the CBP host and was lower when exciplex emission resulted with other hosts. The four examples of exciplexes having λ_{max} shorter than 600 nm each had still fairly high efficiencies, but the efficiency dropped rather suddenly as the λ_{max} became greater than 600 nm. The drop in efficiency with increasing wavelength may in part be a consequence of increased nonradiative decay rates as the gap between the excited state and the ground state decreases (energy gap law).[55]

A device exhibiting the molecular [Cu(PNP-^{t}Bu)]$_2$ emission with CBP as host in the emissive layer was immersed in liquid nitrogen. Figure 7b shows that, like the PL spectrum of the doped TAPC film, the device EL spectrum also shifted between 295 and 77 K. It should be noted that the drive voltage increased substantially at 77 K, and thus the intensity may be affected by concomitant changes in device physics.

OLEDs with electrical leads attached were mounted in a cryostat inside an X-band (9.12 GHz) microwave cavity for electrically detected electron paramagnetic resonance (EDEPR) experiments. While the $g = 2$ region in such experiments on operating OLEDs is swamped by organic radicals and there is little resolution among species, the EDEPR spectra of the triplet species are distinctive. In particular, triplet signals from different species in the half-field region comprising $m_s = -1 \leftrightarrow m_s = +1$ transitions of triplet states may be resolved because of the differences in the ZFS among the materials. Figure 8a shows the EDEPR spectra at 15 K in the half-field region of devices with and without [Cu(PNP-^{t}Bu)]$_2$ dopant in the CBP host. In a prior study,[34] the resonances from the CBP host, the Bphen electron-transport material, and the NPB hole-transport material were identified in the undoped device. In the doped device, the Bphen triplet signal was eliminated, consistent with the holes being trapped by the dopant and prevented from reaching the Bphen layer where some portion of the recombination could otherwise occur. The CBP and NPB triplet signals were also strongly reduced in the doped device, showing that the triplet excitons were strongly partitioned to the dopant. A new signal at 160 mT was observed in the doped device. This signal was observed in doped devices with the TCTA host as well. Moreover, it was also observed when the magnetic resonance was detected optically by the EL. Thus, the new signal is tentatively assigned to the [Cu(PNP-^{t}Bu)]$_2$ dopant.

To optimize the molecular [Cu(PNP-^{t}Bu)]$_2$ electroluminescence, numerous device formulations involving CBP as host were fabricated and tested. These formulations included variations in dopant concentration and placement, additional cohosts, and different materials in electron- and hole-transport layers. The highest efficiency was obtained with CBP and TAPC cohosts and a [Cu(PNP-^{t}Bu)]$_2$ concentration of 0.2%, which is remarkably low compared to the 6 to 8% dopant concentrations typical for phosphorescent OLEDs comprising iridium dopants. The complete device formulation had the following sequence of layers: ITO (220 Å) | CFx (10 Å) | TAPC (750 Å) | CBP + 25% TAPC (100 Å) | CBP + 25% TAPC + 0.2% [Cu(PNP-^{t}Bu)]$_2$ (350 Å) | CBP (100 Å) | BAlq-13 (400 Å) | LiF (5 Å) | Al (1200 Å), where BAlq-13 is bis(2-methyl-quinolin-8-olato)(2,6-diphenylphenolato)aluminum(III).[32] Figure 9a shows the dependence of the efficiency upon current density for this device.

(55) Meyer, T. J. *Pure Appl. Chem.* **1986**, *58*, 1193–1206.

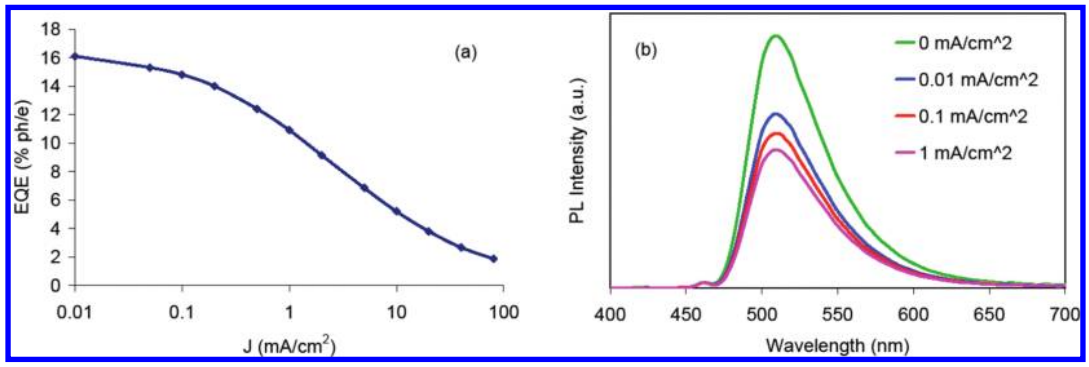

Figure 9. (a) Dependence of external quantum efficiency upon current density for the device: ITO (220 Å) | CFx (10 Å) | TAPC (750 Å) | CBP + 25% TAPC (100 Å) | CBP + 25% TAPC + 0.2% [Cu(PNP-^{t}Bu)]$_2$ (350 Å) | CBP (100 Å) | BAlq-13 (400 Å) | LiF (5 Å) | Al (1200 Å). (b) Dependence of photoluminescence upon applied current density for holes-only device ITO (250 Å) | CFx (10 Å) | TAPC (750 Å) | TAPC + 8% [Cu(PNP-^{t}Bu)]$_2$ (350 Å) | TAPC (500 Å) | Al (1200 Å). The small feature at 460 nm is an artifact of scattered excitation light centered at 450 nm that was incompletely removed by the long-pass cutoff filter shielding the detector.

The maximum EQE of 16.1% (47.5 cd/A) was recorded at 0.01 mA/cm^2. The efficiency decreased with increasing current and reached a value of 10.9% EQE (32 cd/A) at 1 mA/cm^2.

The maximum efficiency of 16.1% may be put in perspective by reference to eq 4, where IQE is the internal quantum efficiency of converting charges passed into photons and Φ_{opt} is the optical outcoupling.

$$EQE = \Phi_{opt} IQE \tag{4}$$

A model based on classical ray optics predicts a maximum possible outcoupling of 22% from these simple bottom-emitting devices supported on glass having an index of refraction of 1.5.[56] Reports of EQE above that limit[12−14] suggest that either the optical model[57] or the measurements need refinement. Nevertheless, the model and the experimental reports give a range to expect for Φ_{opt}, which leads to an estimated range for IQE of the present device of 55−73%. The upper limit of IQE for a phosphorescent emitter would be 100% assuming that all of the excitons from charge recombination are confined to the emitter and its photoluminescence quantum yield is unity, while the IQE of fluorescent OLEDs would be limited to 25% by consideration of the quantum mechanical degeneracy of singlet and triplet spin states. It has been shown that in some devices the 25% statistical limit for singlet excitons may be exceeded via triplet−triplet annihilation to produce additional singlets (sometimes referred to as P-type delayed fluorescence), but the theoretical limit for this process brings the resultant upper limit for singlet excitons only up to 40%.[58] The present device must therefore be harvesting triplet excitons through the dopant and not just singlets.

As shown in Figure 9a, the maximum efficiency occurred at low current density and decreased with increasing current. This efficiency roll-off behavior was exhibited by all other device formulations with CBP or TCTA as host. To probe the origin of the current-dependent roll-off, devices that transport only holes were doped with [Cu(PNP-^{t}Bu)]$_2$. These devices contained the hole-transport material TAPC and had the following structure: ITO (250 Å) | CFx (10 Å) | TAPC (750 Å) | TAPC + x% [Cu(PNP-^{t}Bu)]$_2$ (350 Å) | TAPC (500 Å) | Al (1200 Å), where the dopant concentration x was varied from 0.25 to 8%. No electroluminescence was observed, consistent with devices that transport only holes and in which recombination occurs only at the cathode. However, these devices aided characterization of certain electrical and photophysical properties of the dopant in devices as follows. The device with 1% dopant concentration was subject to ambient light and temperature, and then its cyclic voltammetry was recorded in the dark. In the voltammogram shown in Figure 8b, currents of ±0.09 μA represent capacitive charging of the device, but no injection of holes into the organic layers. The onset of hole injection in the first sweep was observed at 1 V. In the reverse sweep, the charges were not retracted, indicating the charges were deeply trapped. In fact, application of a 10 V reverse bias in the dark took many minutes to detrap charges. In successive sweeps, the onset of charge injection shifted to higher voltage as shown in Figure 8b, consistent with the device already containing trapped charges from the preceding scan. In other experiments, exposure of devices already containing trapped charges to various wavelengths from blue to the NIR resulted in a relatively quick return of the voltage for the onset of charge injection to that of the initial sweep, showing that the trapped holes were readily detrapped by photons.

The PL of the holes-only devices while current was applied was monitored with an excitation band centered at 450 nm to excite the dopant directly. As shown in Figure 9b, the PL intensity was quenched with increasing hole current. When the current was switched off, the PL intensity returned quickly to its initial level with no applied current, consistent with the

(56) Greenham, N. C.; Friend, R. H.; Bradley, D. D. C. *Adv. Mater.* **1994**, *6*, 491–494.
(57) Nowy, S.; Krummacher, B. C.; Frischeisen, J.; Reinke, N. A.; Brütting, W. *J. Appl. Phys.* **2008**, *104*, 12109−1–9.
(58) Kondakov, D. Y. *J. Soc. Info. Display* **2009**, *17*, 137–144.
(59) Harkins, S. B. *The synthesis and study of redox-rich, amido-bridged Cu2N2 dicopper complexes*, Dissertation, California Institute of Technology, 2006 (http://resolver.caltech.edu/CaltechETD:etd-08132005-093856).
(60) Breddels, P. A.; Berdowski, P. A. M.; Blasse, G. *J. Chem. Soc. Faraday Trans.* **1982**, *78*, 595–601.
(61) Zhang, Q.; Zhou, Q.; Cheng, Y.; Wang, L.; Ma, D.; Jing, X.; Wang, F. *Adv. Mater.* **2004**, *16*, 432–436.
(62) Tsuboyama, A.; Kuge, K.; Furugori, M.; Okada, S.; Hoshino, M.; Ueno, K. *Inorg. Chem.* **2007**, *46*, 1992–2001.
(63) Mankad, N. P.; Harkins, S. B.; Antholine, W. E.; Peters, J. C. *Inorg. Chem.* **2009**, *48*, 7026–7032.
(64) Zhang, Q.; Zhou, Q.; Cheng, Y.; Wang, L.; Ma, D.; Jing, X.; Wang, F. *Adv. Funct. Mater.* **2006**, *14*, 1203–1208.
(65) Che, G.; Su, Z.; Li, W.; Chu, B.; Li, M.; Hu, Z.; Zhang, Z. *Appl. Phys. Lett.* **2006**, *89*, 103511−1–3.
(66) Zhang, Q.; Ding, J.; Cheng, Y.; Wang, L.; Xie, Z.; Jing, X.; Wang, F. *Adv. Funct. Mater.* **2007**, *17*, 2983–2990.
(67) Si, Z.; Li, J.; Li, B.; Liu, S.; Li, W. *J. Lum.* **2009**, *129*, 181–186.
(68) Zhang, L.; Li, B.; Su, Z. *J. Phys. Chem. C* **2009**, *113*, 13968–13973.

photodetrapping observed in the voltammetry experiments. Similar CV and EL-PL results were obtained with holes-only devices based on 4,4′,4″-tris[(3-methylphenyl)phenylamino]triphenylamine (MTDATA), except the devices based on this lower oxidation potential transport material were found to detrap in the dark on the order of minutes. The quenching of PL observed in the holes-only devices and the efficiency roll-off observed in EL devices with increasing current, as shown in Figure 9a, may be explained in the same manner by quenching of the excited state by holes and/or dissociation of the excited state under the influence of the electric field. The one-electron oxidized complex, $[Cu(PNP\text{-}^tBu)]_2SbF_6$, was previously isolated,[30] and its absorption spectrum[59] was found to have an extinction of $\sim$2340 M^{-1} cm^{-1} at 515 nm, which is very near to the emission maximum of the neutral $[Cu(PNP\text{-}^tBu)]_2$. Since it was shown that the dopant deeply traps holes, the one-electron oxidation product of the dopant likely makes a significant contribution to the quenching of nearby neutral excited dopant molecules by Förster energy transfer.

Conclusions

The luminescence of $[Cu(PNP\text{-}^tBu)]_2$ arises from two excited states:[60] a triplet and a singlet. The singlet state lies approximately 786($\pm$11) cm^{-1} above the triplet. Emission from the singlet dominates at room temperature, but only emission from the triplet is observed at low temperature. The average observed decay rate of the three triplet sublevels was estimated to be 2913($\pm$75) s^{-1}, and the observed decay rate of the singlet was estimated to be 1.27($\pm$0.09) $\times$ 10^7 s^{-1} by a fit of an expression for a Boltzmann average decay rate to the temperature dependence of the observed overall decay rates of a doped film. Assuming that the quantum yield in the doped film is the same as that in solution (57%) leads to radiative rate constants of 1.66 $\times$ 10^3 s^{-1} for the triplet and 7.24 $\times$ 10^6 s^{-1} for the singlet.

The distinguishing properties of $[Cu(PNP\text{-}^tBu)]_2$, $[Cu(PNP)]_2$, and related mononuclear amidophosphine Cu(I) complexes are the quantum yields in solution,[29,31] which are higher than those of any other copper(I) complexes or any systems exhibiting E-type delayed fluorescence of which we are aware. There are some reports of Cu(I) complexes having much higher quantum yields in the solid state rather than solution.[61,62] The Stokes shift at room temperature for $[Cu(PNP\text{-}^tBu)]_2$ ($\sim$2070 cm^{-1}) is much smaller than those in previously studied Cu(I) phenanthroline complexes, including $Cu(dmp)^{2+}$ ($\sim$7390 cm^{-1})[23] and Cu(dmp)(bis(2-(diphenylphosphino)phenyl)ether)$^+$ ($\sim$8410 cm^{-1}).[26] The relatively small Stokes shift indicates less distortion in the excited state of $[Cu(PNP\text{-}^tBu)]_2$, thereby reducing nonradiative decay pathways and resulting in the high quantum yield. The TD-DFT calculations also predicted little structural change in the excited state. This view of the excited state geometry is complementary to the XAS,[30] X-ray,[29] and EPR[63] studies that indicated little structural change upon oxidation of HOMO that is highly delocalized over the $Cu_2(\mu\text{-}NAr_2)_2$ core with a substantial contribution from the N lone pairs.

When $[Cu(PNP\text{-}^tBu)]_2$ was doped into vapor-deposited OLEDs, broad red-shifted electroluminescence attributed to exciplexes was obtained with many of the materials screened as hosts, whereas green EL was obtained with host materials such as CBP having sufficiently high LUMO levels. The CV of holes-only devices showed that the dopant deeply traps holes, implying that recombination occurs directly on the dopant in EL devices, immediately producing trapped singlet or triplet excitons. The EDEPR of devices with the CBP host further showed that triplet excitons are strongly partitioned to the $[Cu(PNP\text{-}^tBu)]_2$ dopant. At low temperature, EL from the triplet state was observed. Although the luminance efficiency at 295 K dropped as the current density increased in these devices, the high efficiency of 16.1% EQE, measured at low current density, confirms the conclusion that the $[Cu(PNP\text{-}^tBu)]_2$ devices must not be limited to harvesting only singlet excitons but must also be harvesting triplet excitons. There has been one other report of light-emitting electrochemical cells based on neat films of ionic Cu(I) complexes that also gave up to 16% EQE.[64] Unlike OLEDs, however, such devices are of limited utility because they require times on the order of minutes to fully turn on. Prior reports[61,62,65−68] of OLEDs employing copper(I) complexes, many of which were thought to be delayed fluorescence emitters, gave not more than $\sim$5% EQE. The present results demonstrate that it is possible to harvest triplet excitons in OLEDs through an E-type delayed fluorescence channel with high efficiency.

Acknowledgment. The authors thank the National Science Foundation for support through Grant CHE 0616782 under the GOALI Program (Grant Opportunity for Academic Liaison with Industry). We thank the following people for technical assistance and insightful discussions: Ching W. Tang, Kevin Klubek, Shouquan Huo, Viktor Jarikov, Christopher Brown, Michael Landry, Debra Blondell, Shawn Reuter, and Dustin Comfort. We are grateful to Prof. Richard Eisenberg, University of Rochester, who was instrumental in bringing about our collaboration.

Supporting Information Available: Details of DFT calculations and complete ref 46. This material is available free of charge via the Internet at http://pubs.acs.org.

JA1004575